Energy Storage Materials 6 (2017) 112–118

Contents lists available at ScienceDirect

Energy Storage Materials

journal homepage: www.elsevier.com/locate/ensm

Nitrogen and phosphorus codoped hierarchically porous carbon as an efficient sulfur host for Li-S batteries

Wei Ai[a,b], Weiwei Zhou[c], Zhuzhu Du[b], Yu Chen[a], Zhipeng Sun[d], Chao Wu[a,e], Chenji Zou[a], Changming Li[e], Wei Huang[b,f,*], Ting Yu[a,**]

[a] Division of Physics and Applied Physics, School of Physical and Mathematical Sciences, Nanyang Technological University, 637371 Singapore, Singapore
[b] Key Laboratory of Flexible Electronics (KLOFE) & Institue of Advanced Materials (IAM), National Jiangsu Synergistic Innovation Center for Advanced Materials (SICAM), Nanjing Tech University (NanjingTech), 30 South Puzhu Road, Nanjing 211816, China
[c] School of Materials Science and Engineering, Harbin Institute of Technology at Weihai, Weihai 264209, China
[d] Key Laboratory of Materials and Technology for Clean Energy, Ministry of Education, Key Laboratory of Advanced Functional Materials, Xinjiang University, Urumqi, Xinjiang Province, China
[e] Institute for Clean Energy & Advanced Materials, Southwest University, Chongqing 400715, China
[f] Key Laboratory for Organic Electronics & Information Displays (KLOEID) and Institute of Advanced Materials (IAM), Nanjing University of Posts & Telecommunications, Nanjing 210023, Jiangsu, China

ARTICLE INFO

Keywords:
Hierarchically porous carbon
Nitrogen and phosphorus codoping
Sulfur host
Physisorption and chemisorption
Li-S batteries

ABSTRACT

For the first time, nitrogen and phosphorus codoped hierarchically porous carbon (NPHPC) has been explored as an efficient host for sulfur. The material is fabricated based on a scalable, one-step process involving the pyrolysis of melamine polyphosphate synthesized via a simple and versatile organic approach by using low cost industrial raw materials (melamine and polyphosphoric acid). The key features of NPHPC are the hierarchically porous structure and high surface area (1398 $m^2 g^{-1}$) that not only benefit for maximum sulfur loading but also capable of suppressing the dissolution of polysulfides through physisorption. Meanwhile, the N and P codopants together with the thermally stable functionalities are favorable for binding polysulfides via chemisorption. Benefitting from the synergistic effect of structural confinement (physisorption) and chemical binding (chemisorption), the NPHPC/S composite with a high sulfur content of 73 wt% delivers high capacity (1580 mAh g^{-1} at 0.02 C) and long lifespan (200 cycles with 71% retention) for Li-S batteries. The present work highlights the importance of adopting heteroatom-doped hierarchically porous carbon for improving the performance of Li-S batteries, which may further stimulate more efforts in exploring advanced carbon-based hosts in the near future.

1. Introduction

With the over consumption of non-renewable fossil fuels (e.g., coal, petroleum and natural gas) associated with the world energy crisis and climate change, people are searching for reliable and green energy technologies which, in principle, are also crucial for a sustainable world [1]. Wind, solar and hydro energies are exactly the renewable sources. However, these energies are typically intermittent and localized; therefore the development of smart energy storage techniques is essential prior to sufficiently utilizing and easily transporting the energies [2]. Driven by their high gravimetric and volumetric energy densities (~2600 Wh kg^{-1} and ~2800 Wh L^{-1}), Li-S batteries have aroused great research interests in the past few years [3,4]. The fascinating properties of Li-S batteries mainly originate from the high theoretical capacity of sulfur cathode (1672 mAh g^{-1}), which is based on a reversible conversion reaction between sulfur and Li^+ ions to form Li_2S that involves two electrons transfer per sulfur atom [5,6]. Moreover, sulfur is low-cost, environmental friendly and abundant in nature. However, the practical application of Li-S batteries faces the following challenges: (i) Sulfur is a typical insulator with an extremely low conductivity of ~10^{-30} S cm^{-1}, whereas its discharge product Li_2S is also an electro-inactive material with low electronic and ionic conductivities of 10^{-14} and 10^{-13} S cm^{-1}, respectively [7,8]. Therefore, conductive matrix is generally required to ensure an efficient utilization of sulfur. (ii) The intermediate products of sulfur, i.e., lithium polysulfides (Li_2S_n, n≥4), are soluble in the liquid electrolyte,

* Corresponding author at: Key Laboratory of Flexible Electronics (KLOFE) & Institue of Advanced Materials (IAM), National Jiangsu Synergistic Innovation Center for Advanced Materials (SICAM), Nanjing Tech University (NanjingTech), 30 South Puzhu Road, Nanjing 211816, China.
** Corresponding author.
E-mail addresses: wei-huang@njtech.edu.cn (W. Huang), yuting@ntu.edu.sg (T. Yu).

http://dx.doi.org/10.1016/j.ensm.2016.10.008
Received 11 August 2016; Received in revised form 19 October 2016; Accepted 23 October 2016
Available online 26 October 2016

which can shuttle between the anode and cathode during cycling, resulting in some formidable parasitic phenomenons, for example, loss of active material, passivation of Li anode and reduction of coulombic efficiency [9–11]. In addition, the structural and morphological changes of sulfur during cycling lead to poor mechanical stability of the electrode and thus fast capacity fading [4,12].

Aiming to solve the aforementioned problems, intensive research efforts have been devoted to trapping the soluble polysulfides in the cathode region [13]. To date, various kinds of nanostructures, including porous carbons, metal oxides, metal hydroxides and conducting polymers, have been extensively studied as the hosts for sulfur towards Li-S batteries [12,14]. Compared to other host materials, porous carbons are more promising due to their remarkable physicochemical properties, e.g., high surface area, rich porosity and high electronic conductivity. As a consequence, numerous delicate synthetic strategies have been developed for engineering the physical properties of porous carbons with diverse nanostructures, surface areas and porosities for Li-S batteries [15–18]. It should be pointed out that the trapping of polysulfides in pristine porous carbons is based on physisorption via a weak van der Waals interaction, hence only mitigating polysulfides diffusion to some extent. In contrast, doping with N, B, S, P or halogens has been demonstrated to be an effective route to further modulate the structural and electronic properties of carbonaceous materials, leading to a stronger affinity for polysulfides to carbon through additional chemisorption and thus significantly improved performance [19,20]. Note that the binary- and multi-doping may bring about a synergistic improvement in trapping polysulfides, because they are more effective in modulating the physicochemical properties of carbons with respect to non-doping and single atom doping [21,22]. Motivated by this, N,S-codoped [23–25] and N,B-codoped carbons [26] have been applied as efficient cathode materials for Li-S batteries recently, however, the exploration of N and P codoped carbon cathodes has not been reported. To the best of our knowledge, until now, only the N and P codoped graphene has been investigated as a blocking layer for Li-S batteries [27]. Therefore, it is of particular importance to explore whether N and P codoped carbons could stimulate more functions as potential hosts for sulfur.

In this article, for the first time, we report a novel strategy to efficiently trap polysulfides from the synergistic effect of structural confinement (physisorption) and chemical binding (chemisorption) by using nitrogen and phosphorus codoped hierarchically porous carbon (NPHPC). With such design, the micropores and small mesopores are beneficial for encapsulating/immobilizing sulfur, trapping the dissolved polysulfides, and also suppressing the loss of active material. Meanwhile, the large mesopores cooperate with macropores facilitate good electrolyte immersion, whereas the high surface area ($1398\ m^2\ g^{-1}$) and large pore volume ($1.8\ cm^3\ g^{-1}$) ensure maximum sulfur loading. Importantly, the codoped N and P atoms together with the thermally stable functionalities are capable of binding polysulfide species, thus guaranteeing the high utilization of sulfur. As expected, the NPHPC/S composite with a high S content of 73% shows an exceptional performance for Li-S batteries in terms of high initial discharge capacity (1580 mAh g^{-1} at 0.02 C), good rate capability (499 mAh g^{-1} at 5 C) and long cycling stability (200 cycles with 71% retention).

2. Experimental

2.1. Preparation of NPHPC/S composite

The NPHPC was prepared according to our recently reported method [28]. In a typical procedure, 5.04 g of melamine was first dissolved in 400 mL of hot water under stirring, then 5 mL of polyphosphoric acid was injected into the solution. The mixture was kept at 80 °C for 2 h with stirring. The resulting product was collected by centrifugation and washed with deionized water for several times. After that, the product was dried at 100 °C in an electric oven prior to pyrolysis at 900 °C for 2 h under Argon atmosphere to get NPHPC. The NPHPC/S composite was subsequently prepared via a typical melt-diffusion strategy. Briefly, NPHPC and sulfur were ground together with a weight ratio of 3:7 (Caution: the NPHPC powder can easily float in the air due to its ultra-lightweight), and then heated to 155 °C for 12 h in a sealed stainless steel autoclave.

2.2. Characterization

A Zeiss Auriga Dual-Beam FIB/SEM system was used to take the scanning electron microscopy (SEM) and elemental mapping images. X-ray photoelectron spectroscopy (XPS) analysis was performed on an ESCALAB MK II X-ray photoelectron spectrometer with a monochromatic Al Kα as source. A JEM-2100 transmission electron microscope was applied to record the transmission electron microscopy (TEM) images. A Micromeritics ASAP 2020 instrument was used to conduct N_2 adsorption and desorption characterizations at 77 K. Raman spectra were measured on a WITEC CRM200 Raman system with a 532 nm excitation laser. Thermogravimetric analysis (TGA) was performed on a DTG 60H analyzer under N_2 atmosphere with a heating rate of 10 °C min^{-1}. X-ray diffraction (XRD) patterns were recorded on a D8 Advance diffractometer with a Cu Kα radiation.

2.3. Electrochemical characterizations

The electrochemical performance of the NPHPC/S composite was investigated by using CR2032 coin-type cells, which were assembled in an Ar-filled glove box (O_2 and $H_2O < 0.1$ ppm) with pure Li foil as counter electrodes. The electrolyte was composed of 1 mol L^{-1} lithium bis(trifluoromethanesulphonyl)imide in 1:1 (v/v) 1,3-dioxolane and 1,2-dimethoxyethane with 0.2 mol L^{-1} $LiNO_3$ additive. The working electrode was fabricated by coating a N-methyl-2-pyrrolidone based slurry composing 80 wt% of NPHPC/S composite, 10 wt% of carbon black and 10 wt% of polyvinylidene difluoride (PVDF) on an aluminium foil current collector. After that, the electrode was dried in a vacuum oven at 60 °C overnight, punched out with a diameter of 12 mm, and weighed on a highly accurate electronic balance with a readability of 0.01 mg. For one electrode, the mass loading was controlled to be 1.0–1.8 mg with exclusion of carbon black and PVDF, and the specific capacities were calculated based on the weight of sulfur. The cycling and rate performances of the cells were recorded on a NEWARE battery analyzer, while cyclic voltammetry (CV) and electrochemical impedance spectroscopy (EIS) were performed on a CHI 760D electrochemical workstation. The frequency for EIS measurements ranges from 10^5 to 10^{-1} Hz under open circuit conditions with a voltage amplitude of 5 mV.

3. Results and discussion

Fig. 1 displays the scheme for the synthesis of NPHPC/S composite. Briefly, melamine polyphosphate (MPP, chemical structure shown in Fig. 1) was first fabricated by using low-cost industrial raw materials (melamine and polyphosphoric acid), which was then transformed to NPHPC at 900 °C in Argon atmosphere. The obtained NPHPC was then used for implantation of sulfur. SEM images reveal that NPHPC consists of highly curved carbon nanowalls that randomly assembled to form a three-dimensional porous structure (Fig. 2A). TEM and high-resolution TEM (HRTEM) images show the presence of substantial surface defects (e.g., micropores and mesopores) within the carbon nanowalls of NPHPC (Fig. 2B), which originated from the decomposition of MPP precursor during the annealing treatment. Moreover, HRTEM image (inset of Fig. 2B) suggests the sp^2 carbon domains in NPHPC have a short-range order due to the presence of N and P codopants as well as the residual thermally stable surface functionalities, as schematically shown in Fig. 1. The type IV N_2 adsorption and

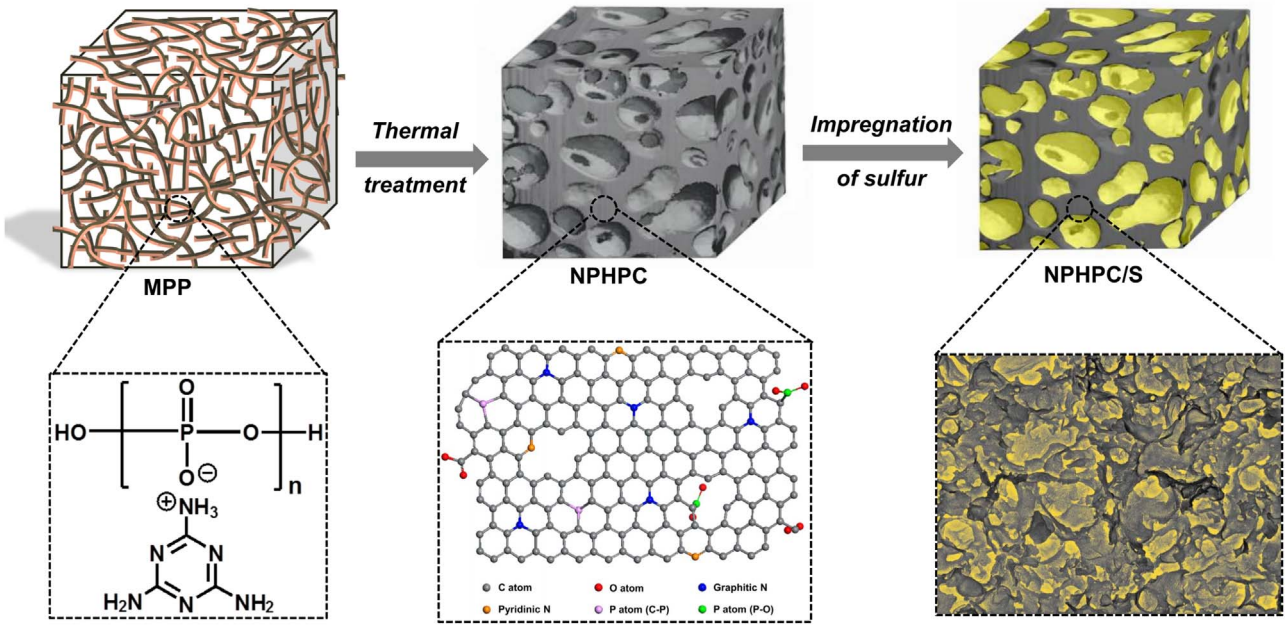

Fig. 1. Schematic illustrating the synthesis of NPHPC and NPHPC/S composite. The MPP was first prepared through a molecular-level design principle, which was subsequently transformed to NPHPC via one-step direct pyrolysis. The final NPHPC was then used as host for sulfur loading via a typical melt-diffusion strategy.

desorption isotherms (Fig. 2C) with well-defined H3 type hysteresis loop of NPHPC, further confirm the coexistence of numerous micropores and mesopores in the sample [29]. Pore size distribution curve shown in the inset of Fig. 2C demonstrates that NPHPC has a hierarchically porous structure with pore sizes ranging from micropores to mesopores and macropores. Such a fascinating porous structure merged with a high surface area of 1398 $m^2 g^{-1}$ and a total pore volume of 1.8 $cm^3 g^{-1}$ ensure NPHPC an ideal storage container for sulfur towards Li-S battery applications (see below). XRD pattern of NPHPC (Fig. 2D) depicts a broad diffraction peak centered at 2θ=24.7°, characteristic of porous carbon nanostructures, indicating its low graphitic nature [30]. Fig. 2E presents the XPS measurements of NPHPC. The signals for P 2p (133.1 eV), P 2s (195.8 eV), C 1s (285.5 eV), N 1s (400.1 eV) and O 1s (531.5 eV) have been clearly detected from the XPS survey spectra. The elemental contents of N and P in NPHPC are calculated to be 2.5 at% and 1.6 at%, respectively. High-resolution N 1s spectrum of NPHPC (Inset in Fig. 2E) reveals the existence of pyridinic N (398.6 eV) and graphitic N (401.5 eV) [31]. While the high-resolution P 2p spectrum (Inset of Fig. 2E) can be deconvoluted into two components of P–C (130.8 eV) and P–O (132.1 eV) bonds [32]. Note that oxygen signal with an elemental content of 11.9 at% is also detected in the XPS survey spectrum of NPHPC (Fig. 2E), which should be ascribed to the residual thermally stable oxygen functionalities. High-resolution O 1s spectrum (Inset of Fig. 2E) discloses that there are two types of oxygen species in NPHPC, that are, C=O (532.4 eV) of carbonyl groups and P=O (530.3 eV) of phosphate groups [33]. It is worth mentioning that both the N and P codopants, and the remaining oxygen containing functional groups can induce charge redistribution (polarization) in NPHPC, thus beneficial for trapping polysulfides through chemical binding between the polarized carbon surfaces and polysulfides [19].

The NPHPC/S composite is prepared by a melt-diffusion strategy as schematically illustrated in Fig. 1. Upon increasing the temperature to 155 °C, the state of sulfur changes from solid to liquid with the lowest viscosity, so that it can be easily captured by the porous structure of NPHPC through capillary forces [5]. SEM images (Fig. 3A–C) display that the resultant composite consists of a vesicle-like structure that is constructed by folded nanowalls. In addition, no bulk sulfur particles are observed, indicating the efficient confinement of sulfur within the internal pore structure of NPHPC. The corresponding elemental mapping images (Fig. 3D and E) suggest sulfur is uniformly distributed in the composite. XRD pattern (Fig. 4A) of NPHPC/S composite shows some orthorhombic phase sulfur peaks (JCPDS No. 08-0247), revealing the presence of crystalline sulfur inside the pores of NPHPC [34]. However, the signals for crystalline sulfur are not observed in the Raman spectrum of NPHPC/S composite (Fig. S1), which is probably caused by the small crystal size of sulfur that is hard to be detected by Raman spectroscopy due to the phonon confinement effect [35,36]. The content of sulfur in the final NPHPC/S composite is determined to be ~73% according to the TGA curve (Fig. 4B).

Fig. 5A shows the CV curves of NPHPC/S composite as a cathode material for Li-S battery. During the cathodic scan, two reduction peaks at ~2.3 and ~2.0 V are observed, corresponding to the reduction of elemental sulfur (S_8) to higher-order Li polysulfides (Li_2S_n, $4 \le n \le 8$) and further reduction of higher-order Li polysulfides to form Li_2S, respectively [37]. Besides, another reduction at ~1.7 V is also detected in the first cycle, which is primarily due to the irreversible reduction of $LiNO_3$ to form a passivating layer on the surface of lithium anode [38]. These results are in agreement with the charge-discharge curves (Fig. S2) and also similar to other reports [39]. In the subsequent reverse sweep of voltage, only one oxidation peak at ~2.4 V is observed that is associated with the oxidation of Li_2S and Li polysulfides into S_8 [37]. The shift of reduction peaks to higher potentials accompanied by the oxidation peak shifts to a lower potential suggest an improved reversibility of the electrochemical reaction upon cycling [37,40]. From the second cycle onwards, the CV curves undergo only slight changes, indicating NPHPC can effectively prevent Li polysulfides from dissolving into the electrolyte because of its unique structure. After an initial activation process at 0.02 C (1 C=1672 mA g^{-1}), the NPHPC/S composite displays stable cycling performance over 200 cycles at a current density of 1 C, as depicted in Fig. 5B. At the low current density of 0.02 C, the NPHPC/S composite delivers a high discharge capacity of 1580 mAh g^{-1} in the first cycle. Note that the capacity below 1.7 V is mainly contributed by the irreversible reduction of $LiNO_3$ [38]. While at the high current density of 1 C, the NPHPC/S composite still possesses an initial discharge capacity of 810 mAh g^{-1}, with 71% capacity remained after 200 cycles, which once again demonstrates the effectiveness of NPHPC in prohibiting the dissolution of Li polysulfides into the electrolyte. Furthermore, the NPHPC/S composite is subjected to cycling at various current densities to evaluate its rate capability (Fig. 5C and D). The

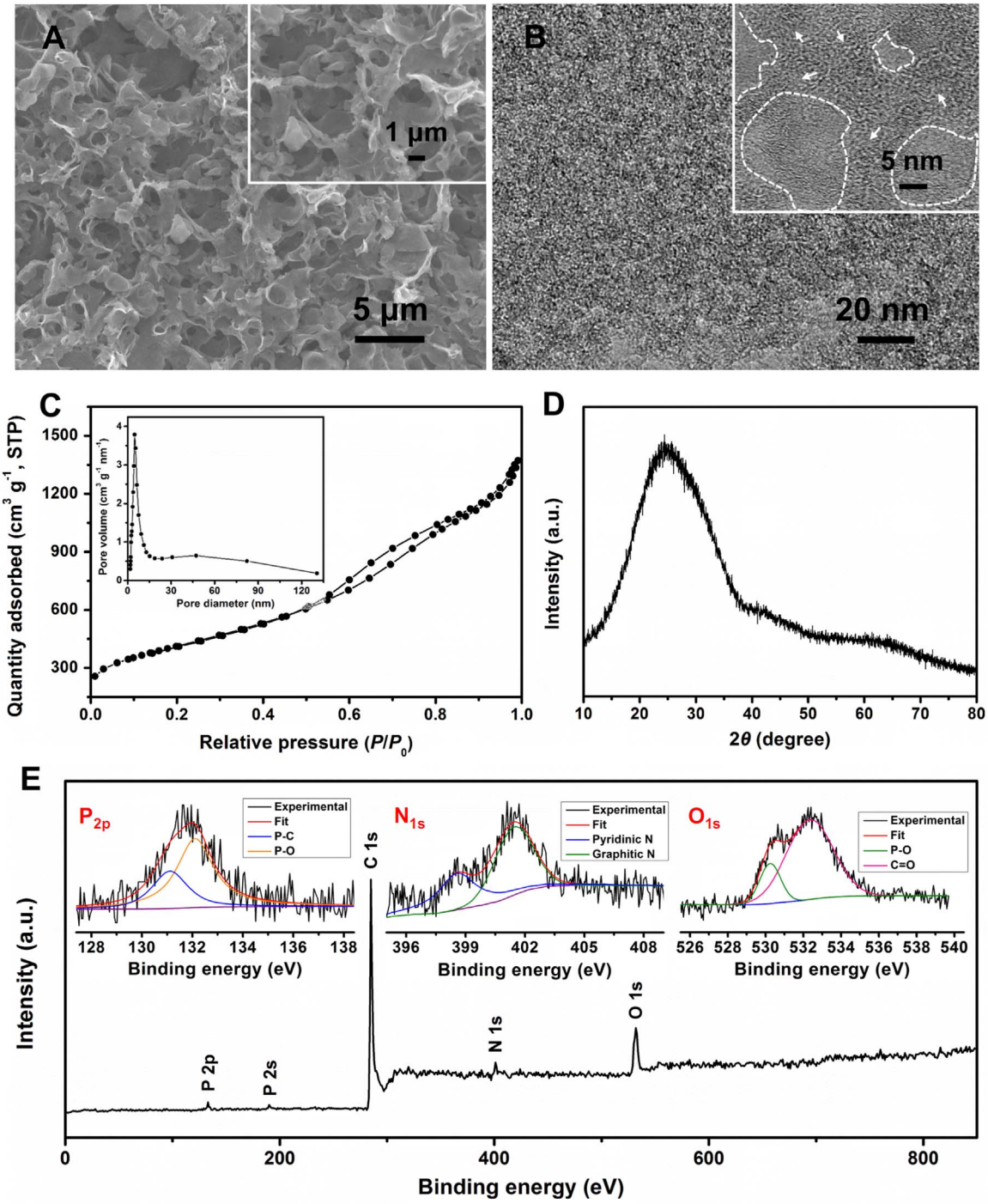

Fig. 2. (A) SEM image of NPHPC. Inset: SEM image of NPHPC with higher magnification. (B) TEM image of NPHPC. Inset: HRTEM image of NPHPC with micropores (< 2 nm diameter, white arrows) and mesopores (2–50 nm diameter, white dotted lines). (C) N_2 adsorption-desorption isotherms of NPHPC at 77 K. Inset: Pore size distribution of NPHPC obtained from the adsorption isotherm using Barrett-Joyner-Halenda method. (D) XRD pattern of NPHPC. (E) XPS survey spectrum of NPHPC. Inset: high resolution P 2p, N 1s and O 1s XPS spectra of NPHPC.

corresponding charge-discharge curves exhibit evident voltage plateaus, that is, two discharge plateaus related to the reduction of S_8 to Li_2S_n (short upper one) and then to Li_2S (long lower one), and one charge plateau refers to the oxidation of Li_2S_n and Li_2S back to S_8 (Fig. 5C). This is consistent with the peaks in previous CV curves (Fig. 5A). It is worth pointing out that the charge-discharge curves still exhibit well-retained voltage plateaus even at very high current densities, which suggests stable electrode kinetics for the redox reactions. With the C rate successively increasing from 0.1 to 0.2, 0.5, 1, 2 and 5 C, the NPHPC/S composite still exhibits stabilized capacity of 887, 775, 689, 633, 578 and 499 mAh g^{-1}, respectively. When the C rate switches back to 0.1 C, the capacity of NPHPC/S composite gradually returns to ~800 mAh g^{-1}, indicative of its good rate capability. For comparison, sulfur with the same content is also impregnated into BP2000 (a commercialized conductive carbon black with a superhigh surface area of 1302 m^2 g^{-1}, Fig. S3A) and N-doped graphene (NG, with a surface area of 504 m^2 g^{-1} (Fig. S3B) that is prepared according to the previously reported method [41]) hosts to form BP2000/S and NG/S composites. The electrochemical properties of BP2000/S and NG/S cathodes in comparison with NPHPC/S are

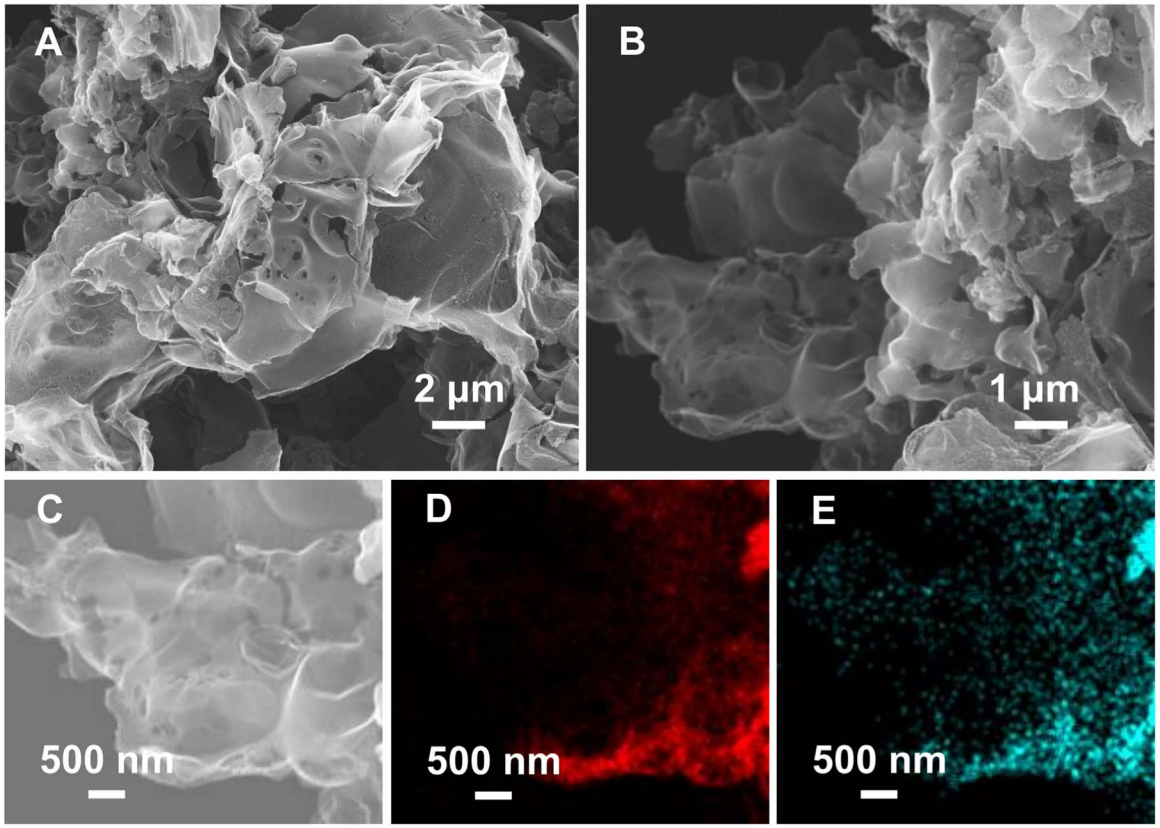

Fig. 3. (A-C) SEM images of NPHPC/S composite at different magnifications. The corresponding elemental mapping images of carbon (D) and sulfur (E) from image (C) reveals the uniform distribution of sulfur in the composite.

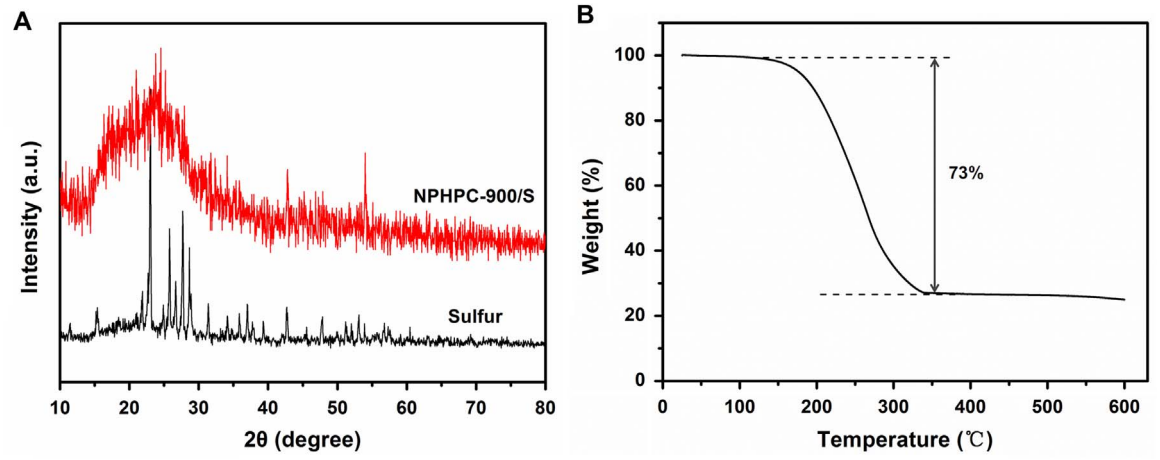

Fig. 4. (A) XRD patterns of sulfur and NPHPC/S composite. (B) TGA profile of NPHPC/S composite between 25 and 600 °C.

shown in Fig. 5B and D. It is evident that the NPHPC/S composite exhibits consistently better electrochemical performances than both BP2000/S and NG/S cathodes, including larger specific capacity, longer cyclic life and superior rate capability, which proves the effectiveness of NPHPC in suppressing the dissolution of polysulfides. In addition, EIS measurements (Fig. S4) reveal that the NPHPC/S composite has a lower charge transfer resistance (R_{CT}=110 Ω) than the BP2000/S (R_{CT}=118 Ω) and NG/S (R_{CT}=130 Ω) electrodes, which verifies an intimate contact between NPHPC and sulfur. On the other hand, the highest slope of NPHPC/S composite in the low frequency range evidences its faster Li^+ ions diffusion inside the electrode [42]. These results are definitely superior to the previously reported carbon-based host materials based on non-doped [43,44] and N-doped porous carbons [45,46], demonstrating NPHPC is a powerful sulfur host for Li-S batteries.

4. Summary

In summary, for the first time, we have demonstrated the application of NPHPC as an efficient sulfur host for Li-S batteries. This well-designed carbon nanoarchitecture is capable of suppressing the dissolution and leakage of polysulfides through coupling the physisorption and chemisorption. Specifically, the hierarchically porous structure of NPHPC is beneficial for trapping polysulfides via physisorption, while the N and P codopants together with the thermally stable oxygen functionalities play a synergistic effect in binding polysulfides via chemisorption, thus leading to sufficient loading and utilization of sulfur. The NPHPC/S composite with a high S loading of 73 wt%

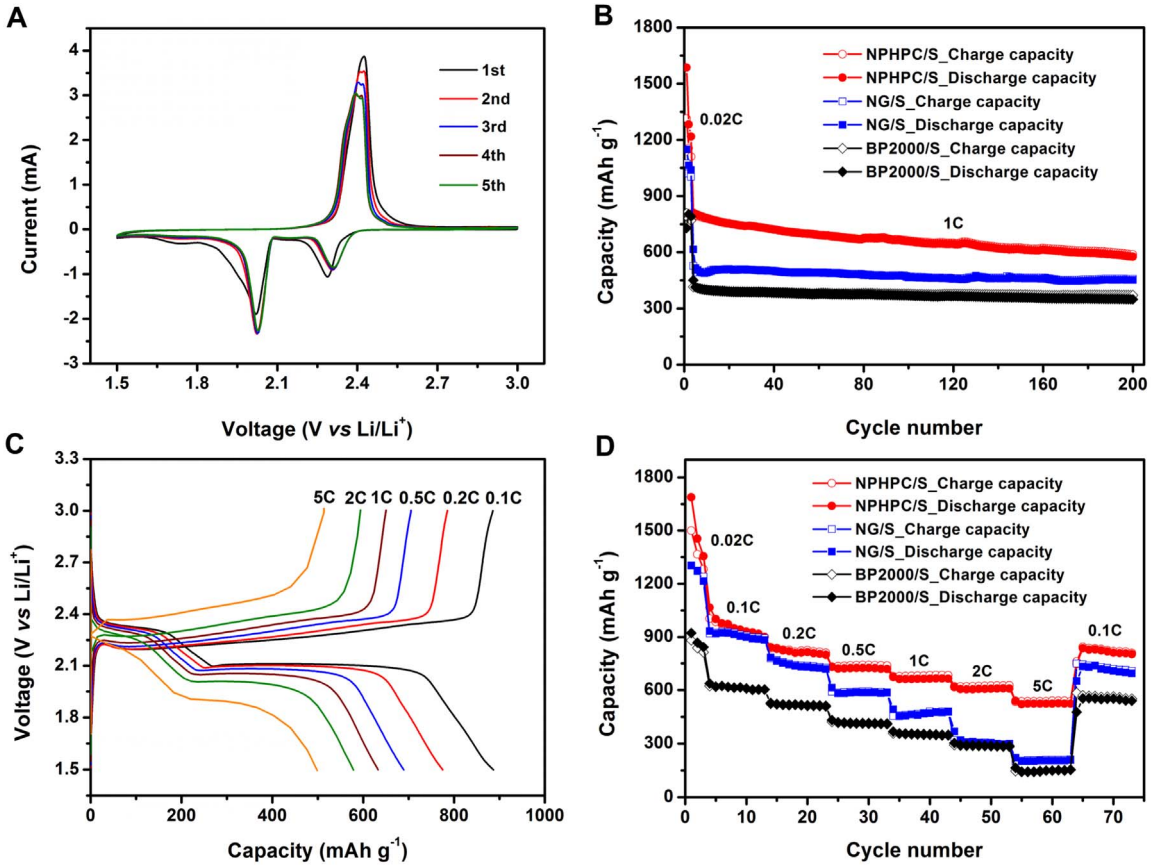

Fig. 5. Electrochemical performances of NPHPC/S composite for Li-S batteries. (A) CV profiles of the NPHPC/S composite electrode at a scan rate of 0.1 mV s^{-1} over a voltage range of 1.5 to 3.0 V (vs. Li/Li^+). (B) Cycling performance of NPHPC/S composite in comparison with the BP2000/S and NG/S electrodes tested at a current density of 1 C after an initial activation process at 0.02 C for three cycles. (C) Galvanostatic charge-discharge curves of NPHPC/S composite electrode cycled at current density increases from 0.1 to 5 C. (D) Rate capability of NPHPC/S, BP2000/S and NG/S electrodes cycled at various current densities.

displays a high initial discharge capacity of 1580 mAh g^{-1} at a current density of 0.02 C and long cycle life at a current density of 1 C with 71% capacity retention over 200 cycles. Moreover, a high capacity of 499 mAh g^{-1} is still retained at the high current density of 5 C, demonstrating the good rate performance of NPHPC/S composite. We believe that our results will enrich the family of carbon-based materials as hosts for sulfur and stimulate further theoretical and experimental efforts on heteroatom-doped carbons for Li-S batteries.

Acknowledgments

This work is supported by A*Star SERC PSF grant 1321202101 and MOE Tier 1 (RG100/15, RG178/15). W.H. thanks the support by the National Basic Research Program of China - Fundamental Studies of Perovskite Solar Cells (2015CB932200), Natural Science Foundation of Jiangsu Province (BM2012010), Priority Academic Program Development of Jiangsu Higher Education Institutions (YX03001), Ministry of Education of China (IRT1148), Synergetic Innovation Center for Organic Electronics and Information Displays, and the National Natural Science Foundation of China (61136003, 51173081). W.Z., and Z.S. thank the support from National Natural Science Foundation of China (21663029, 51502060).

Appendix A. Supporting information

Supplementary data associated with this article can be found in the online version at doi:10.1016/j.ensm.2016.10.008.

References

[1] M.T.H. van Vliet, D. Wiberg, S. Leduc, K. Riahi, Power-generation system vulnerability and adaptation to changes in climate and water resources, Nat. Clim. Change 6 (4) (2016) 375–380.
[2] Z. Yang, J. Zhang, M.C.W. Kintner-Meyer, X. Lu, D. Choi, J.P. Lemmon, et al., Electrochemical energy storage for green grid, Chem. Rev. 111 (5) (2011) 3577–3613.
[3] J. Liang, Z.H. Sun, F. Li, H.M. Cheng, Carbon materials for Li-S batteries: functional evolution and performance improvement, Energy Storage Mater. 2 (2016) 76–106.
[4] Y. Yang, G. Zheng, Y. Cui, Nanostructured sulfur cathodes, Chem. Soc. Rev. 42 (7) (2013) 3018–3032.
[5] X. Ji, K.T. Lee, L.F. Nazar, A highly ordered nanostructured carbon-sulphur cathode for lithium-sulphur batteries, Nat. Mater. 8 (6) (2009) 500–506.
[6] M. Hagen, D. Hanselmann, K. Ahlbrecht, R. Maça, D. Gerber, J. Tubke, Lithium-sulfur cells: the gap between the state-of-the-art and the requirements for high energy battery cells, Adv. Energy Mater. 5 (16) (2015) 1401986.
[7] Z. Lin, C. Liang, Lithium-sulfur batteries: from liquid to solid cells, J. Mater. Chem. A 3 (3) (2015) 936–958.
[8] Y. Son, J.S. Lee, Y. Son, J.H. Jang, J. Cho, Recent advances in lithium sulfide cathode materials and their use in lithium sulfur batteries, Adv. Energy Mater. 5 (16) (2015) 1500110.
[9] J. Wang, Y.S. He, J. Yang, Sulfur-based composite cathode materials for high-energy rechargeable lithium batteries, Adv. Mater. 27 (3) (2015) 569–575.
[10] A. Rosenman, E. Markevich, G. Salitra, D. Aurbach, A. Garsuch, F.F. Chesneau, Review on Li-sulfur battery systems: an integral perspective, Adv. Energy Mater. 5 (16) (2015) 1500212.
[11] R. Xu, J. Lu, K. Amine, Progress in mechanistic understanding and characterization techniques of Li-S batteries, Adv. Energy Mater. 5 (16) (2015) 1500408.
[12] A. Manthiram, S.H. Chung, C. Zu, Lithium-sulfur batteries: progress and prospects, Adv. Mater. 27 (12) (2015) 1980–2006.
[13] A. Manthiram, Y. Fu, Y.S. Su, Challenges and prospects of lithium-sulfur batteries, Acc. Chem. Res. 46 (5) (2013) 1125–1134.
[14] A. Manthiram, Y. Fu, S.H. Chung, C. Zu, Y.S. Su, Rechargeable lithium-sulfur batteries, Chem. Rev. 114 (23) (2014) 11751–11787.
[15] S. Rehman, S. Guo, Y. Hou, Rational design of Si/SiO_2@hierarchical porous carbon spheres as efficient polysulfide reservoirs for high-performance Li-S battery, Adv.

Mater. 28 (16) (2016) 3167–3172.
[16] D.W. Wang, Q. Zeng, G. Zhou, L. Yin, F. Li, H.M. Cheng, et al., Carbon-sulfur composites for Li-S batteries: status and prospects, J. Mater. Chem. A 1 (33) (2013) 9382–9394.
[17] D.W. Wang, G. Zhou, F. Li, K.H. Wu, G.Q. Lu, H.M. Cheng, et al., A microporous-mesoporous carbon with graphitic structure for a high-rate stable sulfur cathode in carbonate solvent-based Li-S batteries, Phys. Chem. Chem. Phys. 14 (24) (2012) 8703–8710.
[18] G. Zhou, S. Pei, L. Li, D.W. Wang, S. Wang, K. Huang, et al., A graphene-pure-sulfur sandwich structure for ultrafast, long-life lithium–sulfur batteries, Adv. Mater. 26 (4) (2014) 625–631.
[19] S.S. Zhang, Heteroatom-doped carbons: synthesis, chemistry and application in lithium/sulphur batteries, Inorg. Chem. Front. 2 (12) (2015) 1059–1069.
[20] A. Vizintin, M. Lozinsek, R.K. Chellappan, D. Foix, A. Krajnc, G. Mali, et al., Fluorinated reduced graphene oxide as an interlayer in Li-S batteries, Chem. Mater. 27 (20) (2015) 7070–7081.
[21] W. Ai, Z. Luo, J. Jiang, J. Zhu, Z. Du, Z. Fan, et al., Nitrogen and sulfur codoped graphene: multifunctional electrode materials for high-performance Li-ion batteries and oxygen reduction reaction, Adv. Mater. 26 (35) (2014) 6186–6192.
[22] J. Liang, Y. Jiao, M. Jaroniec, S.Z. Qiao, Sulfur and nitrogen dual-doped mesoporous graphene electrocatalyst for oxygen reduction with synergistically enhanced performance, Angew. Chem. Int. Ed. 51 (46) (2012) 11496–11500.
[23] S. Niu, W. Lv, G. Zhou, Y. He, B. Li, Q.H. Yang, et al., N and S co-doped porous carbon spheres prepared using l-cysteine as a dual functional agent for high-performance lithium-sulfur batteries, Chem. Commun. 51 (100) (2015) 17720–17723.
[24] Q. Pang, J. Tang, H. Huang, X. Liang, C. Hart, K.C. Tam, et al., A nitrogen and sulfur dual-doped carbon derived from polyrhodanine@cellulose for advanced lithium-sulfur batteries, Adv. Mater. 27 (39) (2015) 6021–6028.
[25] G. Zhou, E. Paek, G.S. Hwang, A. Manthiram, Long-life Li/polysulphide batteries with high sulphur loading enabled by lightweight three-dimensional nitrogen/sulphur-codoped graphene sponge, Nat. Commun. 6 (2015) 8760.
[26] S. Yuan, J.L. Bao, L. Wang, Y. Xia, D.G. Truhlar, Y. Wang, Graphene-supported nitrogen and boron rich carbon layer for improved performance of lithium-sulfur batteries due to enhanced chemisorption of lithium polysulfides, Adv. Energy Mater. 6 (5) (2016) 1501733.
[27] X. Gu, C. j Tong, C. Lai, J. Qiu, X. Huang, W. Yang, et al., A porous nitrogen and phosphorous dual doped graphene blocking layer for high performance Li-S batteries, J. Mater. Chem. A 3 (32) (2015) 16670–16678.
[28] W. Ai, X. Wang, C. Zou, Z. Du, Z. Fan, H. Zhang, et al., Molecular-level design of hierarchically porous carbons codoped with nitrogen and phosphorus capable of in situ self-activation for sustainable energy systems, Small (2016). http://dx.doi.org/10.1002/smll.201602010.
[29] L. Sun, Y. Fu, C. Tian, Y. Yang, L. Wang, J. Yin, et al., Isolated boron and nitrogen sites on porous graphitic carbon synthesized from nitrogen-containing chitosan for supercapacitors, ChemSusChem 7 (6) (2014) 1637–1646.
[30] J. Gu, Z. Du, C. Zhang, S. Yang, Pyridinic nitrogen-enriched carbon nanogears with thin teeth for superior lithium storage, Adv. Energy Mater. 6 (18) (2016) 1600917.
[31] W. Ai, J. Jiang, J. Zhu, Z. Fan, Y. Wang, H. Zhang, et al., Supramolecular polymerization promoted in situ fabrication of nitrogen-doped porous graphene sheets as anode materials for li-ion batteries, Adv. Energy Mater. 5 (15) (2015) 1500559.
[32] M. Latorre-Sanchez, A. Primo, H. Garcia, P-doped graphene obtained by pyrolysis of modified alginate as a photocatalyst for hydrogen generation from water-methanol mixtures, Angew. Chem. Int. Ed. 52 (45) (2013) 11813–11816.
[33] M. Genovese, J. Jiang, K. Lian, N. Holm, High capacitive performance of exfoliated biochar nanosheets from biomass waste corn cob, J. Mater. Chem. A 3 (6) (2015) 2903–2913.
[34] Y. Zhao, W. Wu, J. Li, Z. Xu, L. Guan, Encapsulating MWNTs into hollow porous carbon nanotubes: a tube-in-tube carbon nanostructure for high-performance lithium-sulfur batteries, Adv. Mater. 26 (30) (2014) 5113–5118.
[35] J. Zuo, C. Xu, Y. Liu, Y. Qian, Crystallite size effects on the Raman spectra of Mn_3O_4, Nanostruct. Mater. 10 (8) (1998) 1331–1335.
[36] Q. Zeng, D.W. Wang, K.H. Wu, Y. Li, F. Condi de Godoi, I.R. Gentle, Synergy of nanoconfinement and surface oxygen in recrystallization of sulfur melt in carbon nanocapsules and the related Li-S cathode properties, J. Mater. Chem. A 2 (18) (2014) 6439–6447.
[37] L. Ji, M. Rao, H. Zheng, L. Zhang, Y. Li, W. Duan, et al., Graphene oxide as a sulfur immobilizer in high performance lithium/sulfur cells, J. Am. Chem. Soc. 133 (46) (2011) 18522–18525.
[38] S.S. Zhang, Role of $LiNO_3$ in rechargeable lithium/sulfur battery, Electrochim. Acta. 70 (0) (2012) 344–348.
[39] G. Zhou, L.C. Yin, D.W. Wang, L. Li, S. Pei, I.R. Gentle, et al., Fibrous hybrid of graphene and sulfur nanocrystals for high-performance lithium-sulfur batteries, ACS Nano 7 (6) (2013) 5367–5375.
[40] W. Ai, Z. Du, Z. Fan, J. Jiang, Y. Wang, H. Zhang, et al., Chemically engineered graphene oxide as high performance cathode materials for Li-ion batteries, Carbon 76 (2014) 148–154.
[41] L. Sun, L. Wang, C. Tian, T. Tan, Y. Xie, K. Shi, et al., Nitrogen-doped graphene with high nitrogen level via a one-step hydrothermal reaction of graphene oxide with urea for superior capacitive energy storage, RSC Adv. 2 (10) (2012) 4498–4506.
[42] W. Ai, W. Zhou, Z. Du, C. Sun, J. Yang, Y. Chen, et al., Toward high energy organic cathodes for li-ion batteries: a case study of vat dye/graphene composites, Adv. Funct. Mater. (2016). http://dx.doi.org/10.1002/adfm.201603603.
[43] C. Tang, B.Q. Li, Q. Zhang, L. Zhu, H.F. Wang, J.L. Shi, et al., CaO-templated growth of hierarchical porous graphene for high-power lithium-sulfur battery applications, Adv. Funct. Mater. 26 (4) (2016) 577–585.
[44] B. Papandrea, X. Xu, Y. Xu, C.Y. Chen, Z. Lin, G. Wang, et al., Three-dimensional graphene framework with ultra-high sulfur content for a robust lithium-sulfur battery, Nano Res. 9 (1) (2016) 240–248.
[45] J. Zhang, Y. Cai, Q. Zhong, D. Lai, J. Yao, Porous nitrogen-doped carbon derived from silk fibroin protein encapsulating sulfur as a superior cathode material for high-performance lithium-sulfur batteries, Nanoscale 7 (42) (2015) 17791–17797.
[46] L. Zhou, X. Lin, T. Huang, A. Yu, Nitrogen-doped porous carbon nanofiber webs/sulfur composites as cathode materials for lithium-sulfur batteries, Electrochim. Acta 116 (2014) 210–216.